

ANA LUIZA MENDES¹
DAIMON JEFFERSON JUNG
DE OLIVEIRA²
THAMAYNE VALADARES DE
OLIVEIRA³
FERNANDO AUGUSTO
PEDERSEN VOLL²
RAFAEL BRUNO VIEIRA³
ANDRE BELLIN MARIANO⁴

¹Universidade Federal do
Paraná, Engenharia e Ciência
dos Materiais, Curitiba, Brazil

²Universidade Federal do
Paraná, Engenharia Química,
Curitiba, Brazil

³Universidade Federal de
Uberlândia, Faculdade de
Engenharia Química,
Uberlândia, Brazil

⁴Universidade Federal do
Paraná, Departamento de
Engenharia Elétrica, Curitiba,
Brazil

SCIENTIFIC PAPER

UDC 66.067.1.081:582.26

EFFECTS OF MICROALGAL CONCENTRATION AND pH WITH FLOCCULANT ON MICROFILTRATION

Article Highlights

- Low microalgae concentration and pH were used with flocculant in microfiltration
- The use of flocculant at lower pH can maximize microalgae separation
- Filtration-flocculation was successfully conducted in crossflow filtration

Abstract

*To make algal biomass a suitable feedstock for fuel and bioproducts, a practical way of dewatering and concentrating algal cells must be devised. In this study, a system comprising microfiltration membranes combined with a flocculant was developed on a low-cost ceramic substrate to harvest *Tetrademus obliquus* efficiently. The effects of tannin-based flocculant concentration, microalgal concentration, and pH on microfiltration were studied. Permeate flux was evaluated for 5400 s through experiments to analyze the total resistance and the fouling mechanism. Results show that the cake filtration model best represented the data. The experiments at pH 4 and 0.06 kg/m³ of microalgae (with flocculant) showed improved results with a reduction in the J/J_0 (permeate flux/initial flux) ratio of 39%. In addition, the effects of critical flux, transmembrane pressure, and fouling mechanism on microfiltration were investigated under the best conditions studied. Applying the stepping method to the critical flux yielded a permeate flux of $2.2 \times 10^{-5} \text{ m}^3 \text{ m}^{-2} \text{ s}^{-1}$. The 70 kPa condition showed the highest permeate flux ($3.0 \times 10^{-5} \text{ m}^3 \text{ m}^{-2} \text{ s}^{-1}$) and a low cake pore blocking coefficient (k) obtained by the modified Hermia model. This study showed that Tanfloc at low pH could maximize microalgal separation in membrane processes.*

Keywords: ceramic membrane, concentration, pH, microalgal, microfiltration.

Currently, microalgae have emerged as promising and innovative biomass sources. Microalgae have several applications: biodiesel production, healthy food, fish feed, biohydrogen production, and carbon

dioxide fixation [1]. However, due to the small size of microalgae and their growth in highly dilute conditions, it is important to use an efficient harvest technique [2–4]. Operations currently used in microalgal harvest include centrifugation, sedimentation, flocculation, and membrane filtration [5,6]. Two- or three-step operations in microalgal harvest have been found economical and easily adaptable [7]. For example, a flocculation-sedimentation process combined with membrane filtration has been studied [8–10].

Microalgal harvest through the flocculation-sedimentation process (first step) has already been

Correspondence: T. Valadares de Oliveira, Universidade Federal de Uberlândia, Faculdade de Engenharia Química, 38408-144 Uberlândia, Brazil.

E-mail: thamayne.valadares@ufu.br

Paper received: 25 January, 2022

Paper revised: 16 November, 2022

Paper accepted: 15 December, 2022

<https://doi.org/10.2298/CICEQ220125032M>

studied using various inorganic flocculants such as salts of polyvalent cations like $\text{Al}_2(\text{SO}_4)_3$, $\text{Fe}_2(\text{SO}_4)_3$ and FeCl_3 ; organic flocculants like chitosan, Tanfloc, Flopam, and Zetag [11,12]; and bioflocculants [13].

In particular, Tanfloc is an organic, biodegradable, and nontoxic flocculant (natural polymer). It is a trademark of Tanac (Brazil) and a tannin-based product modified by a physicochemical process. It is obtained from *Acacia mearnsii* and is a high-power flocculant [6,14,15]. Microalgal species, such as *Monoraphidium* sp., showed >90% biomass recovery using 50 mg/L of Tanfloc, while *Scenedesmus* sp. showed $96.7 \pm 1.0\%$ maximum flocculation with a Tanfloc concentration of 210 mg/L [11,16]. However, the relatively high flocculant concentration and the long sedimentation time influence the microalgal purity and processing time, respectively [17].

After flocculation, a dewatering technique (second step) is used for the microalgal slurry to increase the biomass concentration and lower the water content [1]. The flocculation-sedimentation process followed by membrane microfiltration can increase the volume of the processed raw material without significantly increasing the capital cost applied to the project with high microalgal retention [8]. The membrane microfiltration technique effectively solves this problem and is largely acknowledged as an effective separation method [18]. Ceramic membranes have several advantages that enable their use in separation processes: good thermal stability, chemical inertia, high permeability, mechanical strength, long lifetime, and low thermal conductivity [5,19].

Some disadvantages of membrane technologies (microfiltration and ultrafiltration) are reported in the literature, such as fouling and reduced permeate flux over time. These technologies mainly work using the size exclusion principle; therefore, the mechanisms of particle deposition on the surface (external fouling) or in the membrane pores (internal fouling) decrease permeate flux. However, fouling can cause an irreversible loss of membrane permeability, causing operational system failure [20].

Membrane fouling decreases permeate flux, and replacement increases operational and maintenance costs. However, when microfiltration is combined with a flocculation-sedimentation process, they increase the harvest efficiency and reduce the operational and maintenance costs [21,22]. Several control strategies can be applied to prevent fouling, such as pH modification, microalgal concentration, flocculants, and the critical flux concept [14,15]. The critical flux concept has been proposed as a smooth and easy fouling control method that takes advantage of the transition of a filtration system between non-fouling and particle

deposition states by tuning the system flux rate [23,24].

In this study, a flocculation-sedimentation process followed by microfiltration was conducted. The effects of variation in flocculation-sedimentation parameters on microfiltration were evaluated. The flocculation-sedimentation (first step) parameters studied were microalgal concentration, pH, and the presence or absence of Tanfloc (flocculant). Permeate flux, total resistance, the modified Hermia model, and fouling were analyzed during microfiltration (second step). Subsequently, under conditions of minimum fouling, improvement in *Tetradesmus obliquus* microfiltration and fouling management was investigated through the critical flux using the stepping method.

MATERIALS AND METHODS

Microalgae

Microalgae *Tetradesmus obliquus* (GenBank accession number: KY436159.1) were isolated according to Corrêa *et al.* (2017) [25]. The algal was cultivated with Chu medium (mg/L) [25].

Membranes

Faience clay [Cermassas-Pastacer Ltda.] was used as raw material to produce ceramic membranes. Cationic manioc starch grade Superior 300 with a degree of substitution in the range of 0.033–0.036 mol/mol (Grupo Horizonte-Agrícola Horizonte Ltd., PR, Brazil) and eggshell residues were used as additives. Natural clay was modified through thermal treatment at a temperature of 500 °C for 24 h with a heating rate of 5 °C/min. Before thermal treatment, natural clay was dried in an oven for 12 h and dry ground in a bench ball mill. After thermal treatment, the samples were dry ground in a bench ball mill with alumina balls for 4 h and homogenized with a #60 Tyler mesh (2.5×10^{-4} m) sieve. Egg shells were also homogenized using sieving using the same sieve mesh.

A low-cost membrane prepared with cationic starch (2.5% w/w) and eggshell (2.5% w/w) was used [20,26]. The dimensions of the membrane are 0.20 m (length), 1.07×10^{-2} m (internal diameter), and 1.88×10^{-2} m (external diameter) [26]. The membrane properties are the average pore size (1.0 µm), porosity (55%), and flexural strength (15.16 MPa) [26]. Mercury porosimetry was performed on a mercury porosimeter, model Autopore IV 9500 V1.07.

Microfiltration

Water. Hydraulic permeability was conducted to 6.94×10^{-5} m³s⁻¹ and pressure ranging from 20 kPa to 100 kPa and a temperature of 25 °C [5]. Then, the

membrane was compacted with a flux of $6.94 \times 10^{-5} \text{ m}^3 \text{ s}^{-1}$ and a pressure of 100 kPa for 2700 s [5].

Microalgae. Experiments were performed under the conditions of Table 1. The flocculant ratio was 8% w/w (flocculant/microalgae), corresponding to 0.05 kg/m^3 of flocculant per liter of microalgae suspension. These experiments were developed at the pressure of 30 kPa. The microalgae suspension contained 0.06 kg of microalgae/ m^3 . In addition, the permeate flux over time, the retention of microalgae, and the evolution of J/J_0 were analyzed.

Table 1. Microfiltration experiments based on flocculation parameters: microalgal concentration, pH, and presence or absence of flocculant.

Experiment	Microalgae Concentration (kg/m^3)	pH	Flocculant
1	0.02	4	No
2	0.02	7	No
3	0.02	4	Yes
4	0.02	7	Yes
5	0.06	4	No
6	0.06	7	No
7	0.06	4	Yes
8	0.06	7	Yes

Critical flux

According to the results of the previous experiments, the condition used in these tests was 0.06 kg/m^3 at pH 4. The critical flux experiments were done as described elsewhere [27]. The pure water flux was measured at four pressures (squares filled with a straight line) in 600 s intervals. First, pressure increases of 10 kPa were performed. Subsequently, the pressure was decreased at 10 kPa intervals.

Permeate flux

The permeate flux was calculated by Eq. (1):

$$J = \frac{V_p}{A_p t} \quad (1)$$

where V_p is the volume of the permeate (m^3), A_p is the membrane area (m^2), and t is the operating time (s).

Retention of microalgae

The turbidity removal (TUR) was calculated by Eq. (2):

$$TUR(\%) = \frac{T_0 - T_F}{T_0} \quad (2)$$

where T_0 and T_F are the turbidity in the feed and the permeate streams, respectively, in NTU.

Resistance

Total resistance was calculated by Eq. (3):

$$R_T = \frac{TMP}{\mu J} \quad (3)$$

where R_T is the total resistance (m^{-1}), TMP is the transmembrane pressure (kPa), J is the filtration flux ($\text{m}^3 \text{ m}^{-2} \text{ h}^{-1}$), and μ is the dynamic viscosity of water at ($0.8937 \times 10^{-3} \text{ Pa s}$).

Fouling mechanism

The modified Hermia model, Eq. (4), was used [20,28–30].

$$-\frac{dJ}{dt} = k(J_{SS} - J)J^{2-n} \quad (4)$$

The model parameters (k , J_{SS} , and n) were estimated by Eq. (5):

$$OF(k, J_{SS}, n) = \sum_{i=1}^{NE} (J_i^{exp} - J_i^{calc})^2 \quad (5)$$

where J_i^{calc} and J_i^{exp} are calculated and experimental values, NE is the number of experimental points used in the parameter estimation, OF is the objective function, J_i^{calc} is the calculated permeate flux, and J_i^{exp} is the experimental permeate flux.

All simulations, parameter estimation, and statistical analyses were realized in Scilab: using the function `fminsearch` and the Nelder-Mead algorithm. The parameters were calculated according to Bainy *et al.* [31]. The blocking index and its expanded uncertainty (at 95%) were used to identify the most probable fouling mechanism of each membrane [20].

RESULTS AND DISCUSSION

Membrane

The membranes were characterized, and mercury porosimetry showed the pore size distribution from $0.1 \mu\text{m}$ to $8 \mu\text{m}$ (average pore size of $0.82 \mu\text{m}$). Zhou *et al.* (2009) studied an alumina microfiltration membrane modified with nanocrystalline TiO_2 and a pore size of $0.2 \mu\text{m}$ [32]. The small size of some algal cells is typically in the range of 2 mm – 40 mm [33]. Laksono *et al.* [34] concluded that the microalgae form larger aggregates or flocs with the addition of flocculant; thus, less fouling is expected with the flocculated microalgae and also observed that flocculation can be used as a pretreatment before membrane filtration to control fouling.

Flocculation

Tanfloc has an average molecular mass of 1.70 kDa ($2.82 \times 10^{-24} \text{ kg}$) [14]. Due to its high charge

density and low molecular weight, the mechanism of Tanfloc has been suggested to be coagulation [35,36]. The cell surfaces of microalgae have predominantly carboxylic (-COOH) and amine (-NH₂) groups [7]. The carboxylic groups above pH 4–5 are negatively charged, while the amine groups are uncharged [7]. In this study, the pH range studied was 4–7. Positively charged polymers such as Tanfloc neutralize the negative charges; thus, electrostatic repulsion decreases, and aggregates or flakes form [37]. The experiments performed on the membrane showed that the potential is negatively charged in this pH range (4 to 7).

Figure 1 illustrates the flocculation (coagulation mechanism)/microfiltration process of microalgae in nature and flocculated microalgae.

Microalgal concentration and pH

The results of the evolution of (J/J_0) (permeate flux/initial flux) versus time are shown in Figures 2

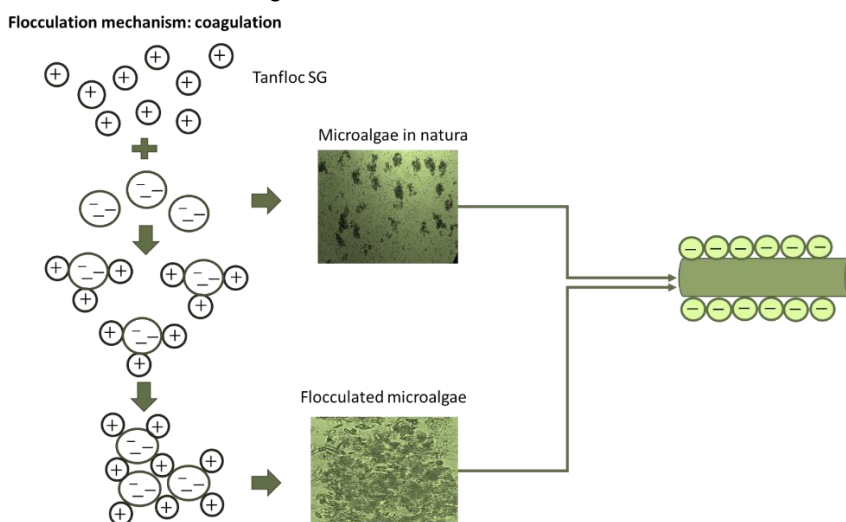


Figure 1. Illustration of the flocculation (coagulation mechanism)/microfiltration process of microalgae in nature and flocculated microalgae.

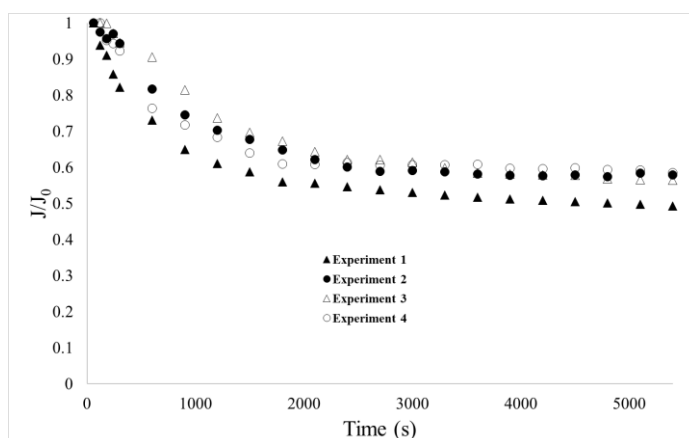


Figure 2. J/J_0 results for 0.02 kg/m³ microalgal concentration and pH (4 and 7).

and 3. For all experiments, the decrease for J/J_0 became stable after 2700 s. However, after the entire process (5400 s of microfiltration), the normalized specific flux decreased by about 40% for the concentration condition of 0.02 kg/m³. Except for experiment 1, which showed the highest reduction J/J_0 (51% reduction). For the experiments with a microalgal concentration of 0.06 kg/m³, the decreases in J/J_0 values were greater than 48%, except for the experiment at pH 4 with flocculant, which showed a 39% reduction. Discart *et al.* [10] studied the dosage of coagulants (FeCl₃ and chitosan) before filtration [10]. Both coagulants increased the filtration efficiency, and they concluded that the coagulant type and dosage should be optimized per membrane.

Figures 4 and 5 show the results of the modified Hermia modeling for the different experimental conditions tested according to Table 1. Figures 4 and 5 show the decline of the flux for the experiments.

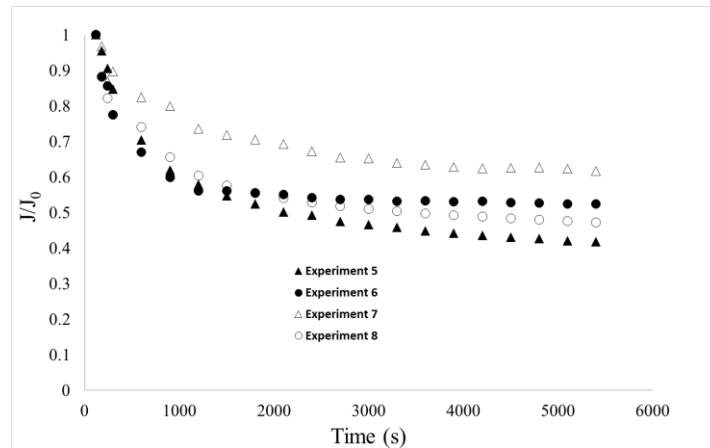


Figure 3. J/J_0 results for 0.06 kg/m^3 microalgal concentration and pH (4 and 7).

The permeate flux decreased slightly with increasing microalgal concentration, as fouling increased when the microalgal concentration increased. The experiments without flocculant increased fouling, as discussed in Membrane.

The cake filtration model provides the best fit (Table 2). The values for the cake blocking coefficient (k) were statistically equal for experiments 1, 2, 4, and 5, while the values obtained for experiments 3, 6, 7, and 8 were statistically different. Laksono *et al.* [34]

observed that the cake filtration model was the most relevant. A similar conclusion was observed by Jiang *et al.* [3].

Turbidity removal of the experiments is shown in Table 3. The turbidity removal varied from 93% to 99%. The experiments with a flocculant (3, 4, 7, and 8) had a higher TUR than the experiments without a flocculant (1, 2, 5, and 6); due to the mechanism of Tanfloc flocculation (coagulation) [35,36].

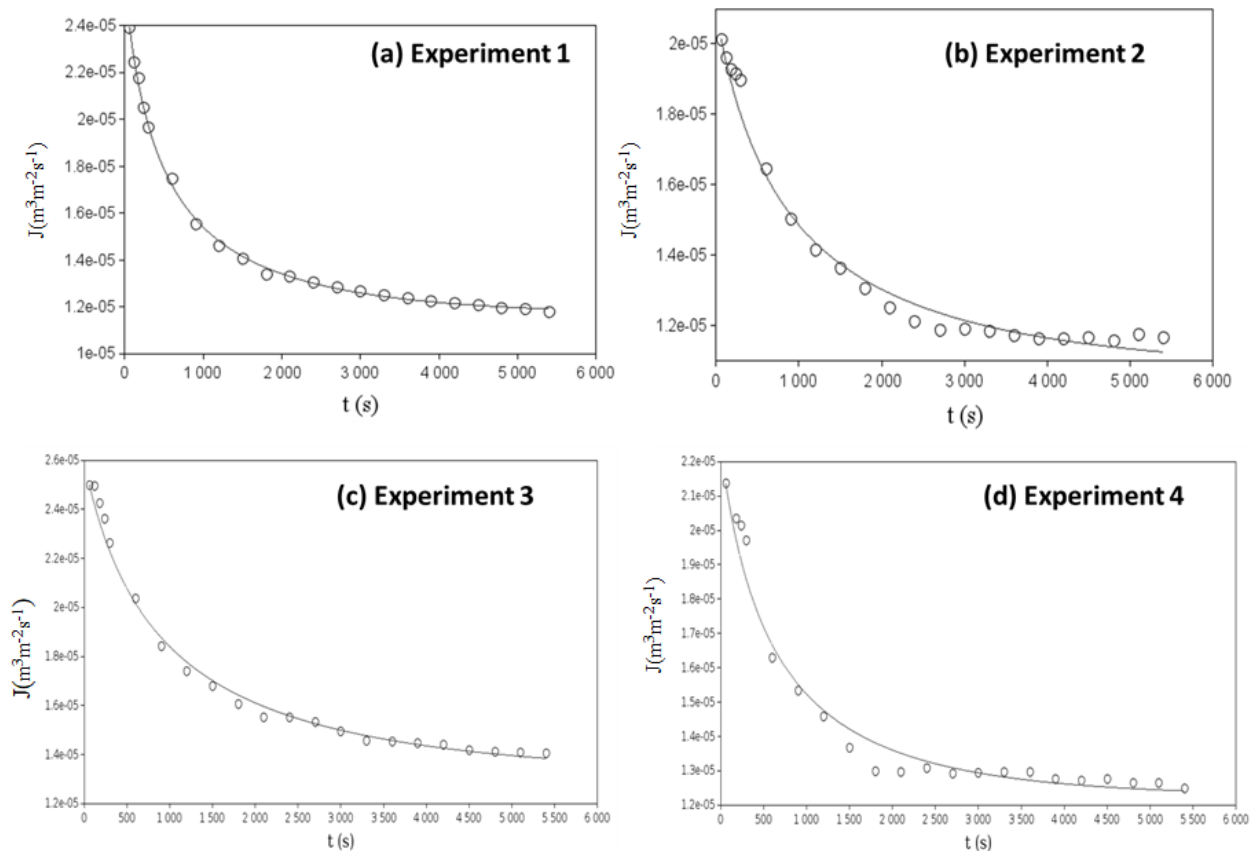


Figure 4. Predictions for the cake models to experiments 1–4 at 30 kPa and 25 °C (lines: estimated results; circles: experimental data).

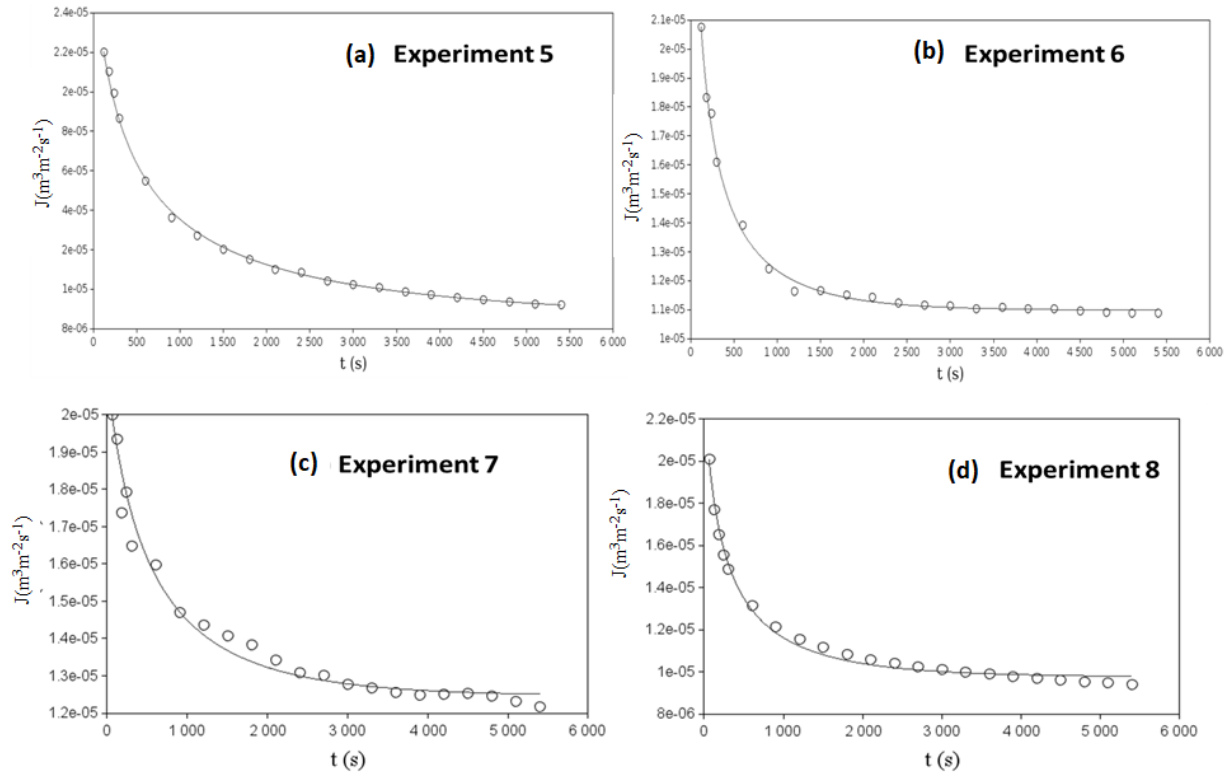


Figure 5. Predictions for the cake models to experiments 5–8 at 30 kPa and 25 °C (lines: estimated results; circles: experimental data).

Table 2. Values for the cake blocking coefficient (*k*).

Experiment	Cake filtration model (n=0) ×10 ⁻⁶	Uncertainty ×10 ⁻⁶
1	3.75	0.2565
2	3.05	0.7475
3	4.06	0.3430
4	10.27	0.9722
5	1.96	0.3839
6	3.90	0.9248
7	5.17	0.1596
8	9.12	0.1427

Table 3. Turbidity removal (%).

Experiment	Turbidity removal (%)	Standard deviation
1	96.4	0.2
2	93.8	0.2
3	97.5	0.3
4	99.1	0.1
5	93.0	0.1
6	94.0	0.2
7	98.1	0.3
8	99.2	0.2

Critical flux

A concentration of 0.06 kg/m³ and pH 4 were chosen. This condition was selected because it showed lower fouling. The results of permeate flux versus pressure for the pressure-stepping method are shown 258

in Figure 6. The water showed higher flux values. The microalgae provided greater fouling. The microalgae permeate flux had a linear increase up to the pressure of 70 kPa. After this pressure, the flux remained almost constant. The critical flux was between 2.11×10⁻⁵ and 2.22×10⁻⁵ m³m⁻²s⁻¹. Increasing the pressure was impossible to increase the flux beyond 2.2522×10⁻⁵ m³m⁻²s⁻¹. The literature divides the critical flux forms into strong and weak [38]. The results with microalgae were in the weak form. There is rapid fouling for the weak form, and the flux-TMP ratio is lower than the pure water line [38]. Due to the membrane characteristics used, the flux values for pure water are much higher than those with microalgae (Figure 6). The literature evaluated critical flux values for different microalgal concentrations and microalgae species ranging from 15 Lm⁻²h⁻¹ to 50 Lm⁻²h⁻¹ [39]. The operating conditions of 30 kPa (below critical flux), 70 kPa (at critical flux), and 100 kPa (above critical flux) were analyzed to evaluate the three regimes shown in Figure 6.

Effect of TMP on filtration behavior

Figure 7 shows (a) the permeate flux at different pressures (30 kPa; 70 kPa; 100 kPa) and (b) J/J₀ at different pressures (30 kPa; 70 kPa; 100 kPa). When Pore blocking is not apparent in a short-term flow test (or TMP), the total filtration resistance keeps constant; because particle accumulation on the membrane surface does not increase significantly. Under these

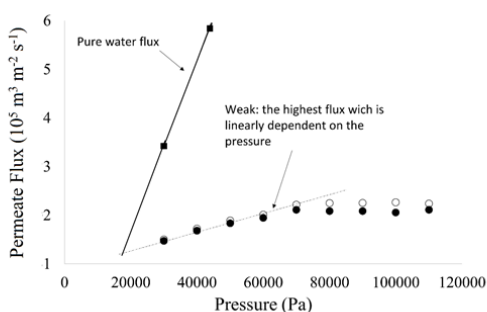
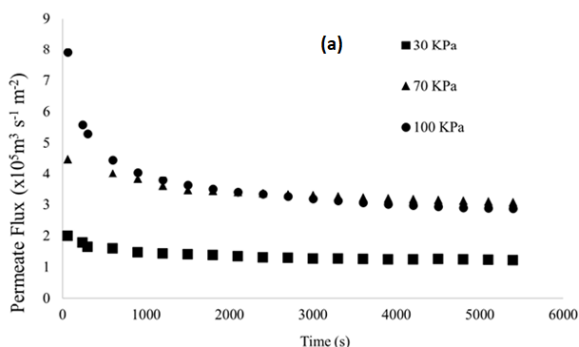


Figure 6. Permeate flux versus pressure for the pressure-stepping method (25°C, pH 4, 0.06 kg/m³).

conditions, the permeate flux increases linearly with TMP. However, if particle accumulation expressively increases with permeate flux, the filtration resistance increases with time, and the permeate flux stop increasing linearly with TMP. Therefore, the breaking point of the linear flow-TMP profile can be considered a critical flux [24]. Based on the results in Figure 7a, higher TMP showed higher initial flux due to the higher driving force. The pressure of 100 kPa potentiated fouling at the membrane surface, resulting in a decline in permeate flux. The permeate flux became stable after 2160 s in the TMP of 70 kPa. The 70 kPa was the condition that showed the best permeate flux results after 5400 s, with a value of $3.05 \times 10^{-5} \text{ m}^3 \text{ m}^{-2} \text{ s}^{-1}$.

The decrease of J/J_0 (Figure 7(b)) was lower at



30 kPa and 70 kPa. TMP at 30 kPa and 70 kPa went through a slow decline stage, and the total decline was almost 39% and 32%, respectively, while at 100 kPa, there was a decrease of 62%. The flux obtained during the subcritical regime does not show a significant drop with time, while the supercritical regime shows a significant drop [3,40]. In this study, the critical flux was at 70 kPa. The membranes under subcritical conditions had superior antifouling performance, but the 70 kPa pressure performed close to the 30 kPa condition.

The total resistance was dependent on the pressure. The results show that the total fouling resistance increased with permeate volume/filtration area (Figure 8). The membranes at 70 kPa had the lowest total resistance and highest permeate volume/filter area. Operation at pressures below the critical flux is favorable for controlling membrane fouling [41]. Methodologies have been widely studied to reduce microalgae harvesting costs to promote economic viability. The cake pore blocking coefficient (k) (Table 4) at lower pressure is higher than for higher pressures (70 kPa and 100 kPa).

It can be seen from Table 4 that at low pressure, there was a significantly higher coefficient, while at critical pressure, it had the lowest coefficient. It was observed in this work that the most relevant factors were the concentration and pH, and at a concentration of 0.06 kg/m^3 , there was a greater reduction of J/J_0 , which represented greater fouling.

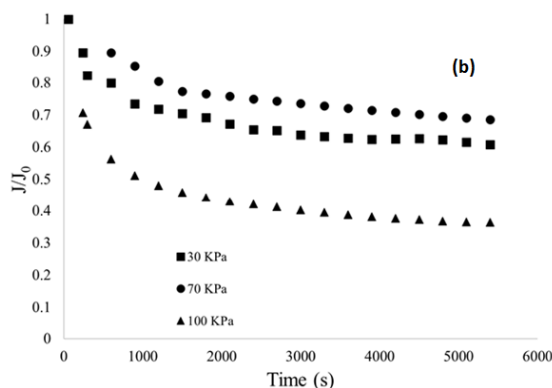


Figure 7. (a) Permeate flux at different pressures; (b) J/J_0 at different pressures.

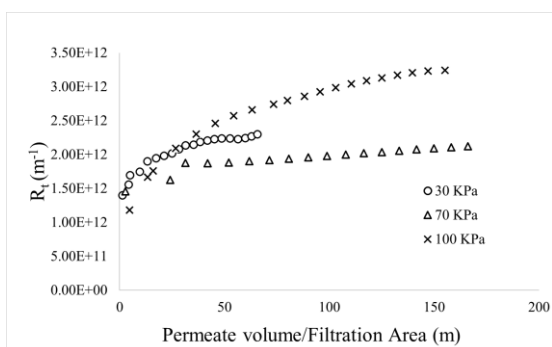


Figure 8. (a) Total fouling resistance with the variation of permeate volume/Filtration area (V/A).

Table 4. Estimated parameters of the model.

Pressure (kPa)	Cake filtration model ($n=0$) $\times 10^{-6}$	Uncertainty $\times 10^{-6}$
30	4.43	0.4327
70	0.46	0.0660
100	0.71	0.0762

CONCLUSION

The flocculation-sedimentation process followed by microfiltration was investigated, and the conclusions are:

The membranes were characterized, and mercury porosimetry showed the pore size distribution from 0.1 to 8 μm (average pore size of 0.82 μm).

The experiments at pH 4 and 0.06 $\text{kg}\cdot\text{m}^{-3}$ of microalgae (with flocculant) showed improved results with a reduction in the J/J_0 ratio of 39%, demonstrating the potential of flocculation to control fouling.

The results of the modified Hermia modeling showed that the cake filtration model best represented the data, which was expected because Tanfloc promotes aggregate or floc formation through coagulation. Therefore, the turbidity removal rate varied from 93% to 99%.

The membranes (0.06 $\text{kg}\cdot\text{m}^{-3}$ and pH 4 with flocculant) in the critical regime had better antifouling characteristics than those in the supercritical and subcritical regimes. Applying the stepping method to the critical flux yielded permeate flux of $2.2\times 10^{-5} \text{ m}^3\text{m}^{-2}\text{s}^{-1}$. The 70 kPa condition showed the highest permeate flux ($3.0\times 10^{-5} \text{ m}^3\text{m}^{-2}\text{s}^{-1}$) and a low cake pore blocking coefficient (k) obtained by the modified Hermia model.

The filtration-flocculation process showed promising results in crossflow microfiltration, verifying the strong interaction between filtration and flocculation.

ACKNOWLEDGEMENT

The authors thank the Brazilian National Council of Scientific and Technological Development - CNPq (Grant 425125/2018-1) and Araucaria Foundation - Support for Scientific and Technological Development of Paraná. They also thank the Federal University of Paraná (UFPR) and the Technology Sector from UFPR for infrastructural support.

NOMENCLATURE

Symbols

J	permeate flux ($\text{m}^3\text{m}^{-2}\text{s}^{-1}$)
V	permeate volume (m^3)
A	membrane area (m^2)
t	operating time (s).
TUR	turbidity removal (%)
T	turbidity (NTU)
R	resistance (m^{-1})
TMP	transmembrane pressure (kPa)
k	resistance coefficient
n	blocking index
OF	objective function

J/J_0 normalized specific flux

Greek letters

M viscosity (Pa s)

Subscripts

p Permeate

F streams

0 feed

T total

Ss steady-state

REFERENCES

- [1] K.H. Min, D.H. Kim, M. Ki, S.P. Pack, *Bioresour. Technol.* (2021) 126404. <https://doi.org/10.1016/j.biortech.2021.126404>.
- [2] M.K. Danquah, L. Ang, N. Uduman, N. Moheimani, G.M. Forde, *J. Chem. Technol. Biotechnol.* 84 (2009) 1078–1083. <https://doi.org/10.1002/jctb.2137>.
- [3] S. Jiang, Y. Zhang, F. Zhao, Z. Yu, X. Zhou, H. Chu, *Algal Res.* 35 (2018) 613–623. <https://doi.org/10.1016/j.algal.2018.10.003>.
- [4] Z. Zhao, A. Ilyas, K. Muylaert, I.F.J. Vankelecom, *Bioresour. Technol.* 309 (2020) 123367. <https://doi.org/10.1016/j.biortech.2020.123367>.
- [5] J.D. de Oliveira Henriques, M.W. Pedrassani, W. Klitzke, A.B. Mariano, J.V.C. Vargas, R.B. Vieira, *Appl. Clay Sci.* 150 (2017) 217–224. <https://doi.org/10.1016/j.clay.2017.09.017>.
- [6] R.H.R. Hanashiro, C.B. Stoco, T. V de Oliveira, M.K. Lenzi, A.B. Mariano, R.B. Vieira, *Can. J. Chem. Eng.* 0 (2019). <https://doi.org/10.1002/cjce.23467>.
- [7] D. Vandamme, I. Foubert, K. Muylaert, *Trends Biotechnol.* 31 (2013) 233–239. <https://doi.org/10.1016/j.tibtech.2012.12.005>.
- [8] Z. Zhao, K. Muylaert, I.F.J. Vankelecom, *Water Res.* 198 (2021) 117181. <https://doi.org/10.1016/j.watres.2021.117181>.
- [9] Z. Zhao, Y. Li, K. Muylaert, I.F.J. Vankelecom, *Sep. Purif. Technol.* 240 (2020) 116603. <https://doi.org/10.1016/j.seppur.2020.116603>.
- [10] V. Discart, M.R. Bilad, R. Moorkens, H. Arafat, I.F.J. Vankelecom, *Algal Res.* 9 (2015) 55–64. <https://doi.org/10.1016/j.algal.2015.02.029>.
- [11] F. Roselet, D. Vandamme, M. Roselet, K. Muylaert, P.C. Abreu, *Bioenergy Res.* 10 (2017) 427–437. <https://doi.org/10.1007/s12155-016-9806-3>.
- [12] A.I. Barros, A.L. Gonçalves, M. Simões, J.C.M. Pires, *Renew. Sustain. Energy Rev.* 41 (2015) 1489–1500. <https://doi.org/10.1016/j.rser.2014.09.037>.
- [13] G. Kandasamy, S.R.M. Shaleh, *Appl. Biochem. Biotechnol.* 182 (2017) 586–597. <https://doi.org/10.1007/s12010-016-2346-7>.
- [14] N.F.H. Selesu, T. V. de Oliveira, D.O. Corrêa, B. Miyawaki, A.B. Mariano, J.V.C. Vargas, R.B. Vieira, *Can. J. Chem. Eng.* 94 (2016) 304–309. <https://doi.org/10.1002/cjce.22391>.
- [15] T. Nishimura, G.V. Garcia Lesak, L. Alves Xavier, R. Bruno Vieira, A. Bellin Mariano, *Chem. Eng. Technol.* 45 (2022) 230–237. <https://doi.org/10.1002/ceat.202100490>.
- [16] R. Gutiérrez, F. Passos, I. Ferrer, E. Uggetti, J. García, *Algal Res.* 9 (2015) 204–211. <https://doi.org/10.1016/j.algal.2015.03.010>.
- [17] C. Wan, M.A. Alam, X.Q. Zhao, X.Y. Zhang, S.L. Guo, S.H. Ho, J.S. Chang, F.W. Bai, *Bioresour. Technol.* 184 (2015) 251–257. <https://doi.org/10.1016/j.biortech.2014.11.081>.

- [18] M. Mouiya, A. Abourriche, A. Bouazizi, A. Benhammou, Y. El Hafiane, Y. Abouliatim, L. Nibou, M. Oumam, M. Ouammou, A. Smith, H. Hannache, *Desalination*. 427 (2018) 42–50. <https://doi.org/10.1016/j.desal.2017.11.005>.
- [19] J.D.D.O. Henriques, M.W. Pedrassani, W. Klitzke, T.V. De Oliveira, P.A. Vieira, A.B. Mariano, R.B. Vieira, *Rev. Mater.* 24 (2019). <https://doi.org/10.1590/s1517-707620190004.0826>.
- [20] W. de Melo, G.V.G. Lesak, T.V. de Oliveira, F.A.P. Voll, A.F. Santos, R.B. Vieira, *Mater. Res.* 25 (2022). <https://doi.org/10.1590/1980-5373-mr-2021-0365>.
- [21] F. Wicaksana, A.G. Fane, P. Pongpairoj, R. Field, *J. Memb. Sci.* 387-388 (2012) 83–92. <https://doi.org/10.1016/j.memsci.2011.10.013>.
- [22] G. Singh, S.K. Patidar, *J. Environ. Manage.* 217 (2018) 499–508. <https://doi.org/10.1016/j.jenvman.2018.04.010>.
- [23] M.T. Alresheedi, O.D. Basu, B. Barbeau, *Chemosphere*. 226 (2019) 668–677. <https://doi.org/10.1016/j.chemosphere.2019.03.188>.
- [24] J. Luo, S.T. Morthensen, A.S. Meyer, M. Pinelo, *J. Memb. Sci.* 469 (2014) 127–139. <https://doi.org/10.1016/j.memsci.2014.06.024>.
- [25] D.O. Corrêa, B. Santos, F.G. Dias, J.V.C. Vargas, A.B. Mariano, W. Balmant, M.P. Rosa, D.C. Savi, V. Kava, C. Glienke, J.C. Ordonez, *Int. J. Hydrogen Energy*. 42 (2017) 21463–21475. <https://doi.org/10.1016/j.ijhydene.2017.05.176>.
- [26] L.A. Xavier, T.V. de Oliveira, W. Klitzke, A.B. Mariano, D. Eiras, R.B. Vieira, *Appl. Clay Sci.* 168 (2019) 260–268. <https://doi.org/10.1016/j.clay.2018.11.025>.
- [27] M. Mänttari, M. Nyström, *J. Memb. Sci.* 170 (2000) 257–273. [https://doi.org/10.1016/S0376-7388\(99\)00373-7](https://doi.org/10.1016/S0376-7388(99)00373-7).
- [28] B.G. Choobar, M.A. Alaei Shahmirzadi, A. Kargari, M. Manouchehri, *J. Environ. Chem. Eng.* 7 (2019) 103030. <https://doi.org/10.1016/j.jece.2019.103030>.
- [29] M.J. Corbatón-Báguena, M.C. Vincent-Vela, J.M. Gozálvarez-Zafrilla, S. Álvarez-Blanco, J. Lora-García, D. Catalán-Martínez, *Sep. Purif. Technol.* 170 (2016) 434–444. <https://doi.org/10.1016/j.seppur.2016.07.007>.
- [30] M.C. Vincent Vela, S. Álvarez Blanco, J. Lora García, E. Bergantiños Rodríguez, *Chem. Eng. J.* 149 (2009) 232–241. <https://doi.org/10.1016/j.cej.2008.10.027>.
- [31] E.M. Bainy, E.K. Lenzi, M.L. Corazza, M.K. Lenzi, *Therm. Sci.* 21 (2017) 41–50. <https://doi.org/10.2298/TSCI160422241B>.
- [32] J. Zhou, X. Zhang, Y. Wang, X. Hu, A. Larbot, *Desalination*. 235 (2009) 102–109. <https://doi.org/10.1016/j.desal.2008.01.013>.
- [33] L. Brennan, P. Owende, *Renew. Sustain. Energy Rev.* 14 (2010) 557–577. <https://doi.org/10.1016/j.rser.2009.10.009>.
- [34] S. Laksono, I.M.A. ElSherbiny, S.A. Huber, S. Panglisch, *Chem. Eng. J.* 420 (2021) 127723. <https://doi.org/10.1016/j.cej.2020.127723>.
- [35] H. Salehizadeh, N. Yan, *Biotechnol. Adv.* 32 (2014) 1506–1522. <https://doi.org/10.1016/j.biotechadv.2014.10.004>.
- [36] U. Suparmaniam, M. Kee, Y. Uemura, J. Wei, K. Teong, S. Hoong, *Renew. Sustain. Energy Rev.* 115 (2019) 109361. <https://doi.org/10.1016/j.rser.2019.109361>.
- [37] M.R. Bilad, V. Discart, D. Vandamme, I. Foubert, K. Muylaert, I.F.J. Vankelecom, *Bioresour. Technol.* 138 (2013) 329–338. <https://doi.org/10.1016/j.biortech.2013.03.175>.
- [38] R.W. Field, D. Wu, J.A. Howell, B.B. Gupta, *J. Memb. Sci.* 100 (1995) 259–272. [https://doi.org/10.1016/0376-7388\(94\)00265-Z](https://doi.org/10.1016/0376-7388(94)00265-Z).
- [39] T. De Baerdemaeker, B. Lemmens, C. Dotremont, J. Fret, L. Roef, K. Goiris, L. Diels, *Bioresour. Technol.* 129 (2013) 582–591. <https://doi.org/10.1016/j.biortech.2012.10.153>.
- [40] P. Le Clech, B. Jefferson, I.S. Chang, S.J. Judd, *J. Memb. Sci.* 227 (2003) 81–93. <https://doi.org/10.1016/j.memsci.2003.07.021>.
- [41] R.W. Field, G.K. Pearce, *Adv. Colloid Interface Sci.* 164 (2011) 38–44. <https://doi.org/10.1016/j.cis.2010.12.008>.

ANA LUIZA MENDES¹
DAIMON JEFFERSON JUNG
DE OLIVEIRA²
THAMAYNE VALADARES DE
OLIVEIRA³
FERNANDO AUGUSTO
PEDERSEN VOLL²
RAFAEL BRUNO VIEIRA³
ANDRE BELLIN MARIANO⁴

¹Universidade Federal do
Paraná, Engenharia e Ciência
dos Materiais, Curitiba, Brazil

²Universidade Federal do
Paraná, Engenharia Química,
Curitiba, Brazil

³Universidade Federal de
Uberlândia, Faculdade de
Engenharia Química, Uberlândia,
Brazil

⁴Universidade Federal do
Paraná, Departamento de
Engenharia Elétrica, Curitiba,
Brazil

NAUČNI RAD

EFEKTI KONCENTRISANJA MIKROALGI SA FLOKULANTOM I pH NA MIKROFILTRACIJU

Da bi biomasa algi postala pogodna sirovina za gorivo i bioproizvode, mora se osmisliti praktičan način njenog dehidratiranja i koncentrisanja. U ovom radu je razvijen sistem koji se sastoji od jeftinih keramičkih mikrofiltracionih membrana kombinovanih sa flokulantom, kako bi se efikasno sakupio Tetrademus obliquus. Proučavani su efekti koncentracije flokulanta na bazi tanina, koncentracije mikroalgi i pH na mikrofiltraciju. Tok permeata je procenjen tokom 90 min kroz eksperimente radi analize ukupnog otpora i mehanizma začepjenja. Rezultati pokazuju da model filtracione pogače najbolje predstavlja podatke. Eksperimenti pri pH 4 i 0,06 kg/m³ mikroalgi (sa flokulantom) pokazali su poboljšane rezultate sa smanjenjem odnosa J/J₀ (fluks permeata/početni fluks) od 39%. Pored toga, istraženi su efekti kritičnog fluksa, transmembranskog pritiska i mehanizma začepjenja na mikrofiltraciju u najboljim uslovima. Primenom metode koraka na kritični fluks dobijen je fluks permeata od $2,2 \times 10^{-5} \text{ m}^3\text{m}^{-2}\text{s}^{-1}$. Pri pritisku od 70 kPa postignut je najveći fluks permeata ($3,0 \times 10^{-5} \text{ m}^3\text{m}^{-2}\text{s}^{-1}$) i nizak koeficijent blokiranja pora pogače (k) dobijen modifikovanim Hermia modelom. Ovaj rad je pokazao da Tanfloc pri niskom pH može maksimizirati odvajanje mikroalgi u membranskim procesima.

Ključne reči: keramička membrana, koncentracija, pH, mikroalge, mikrofiltracija.